Hindawi
Journal of Spectroscopy
Volume 2017, Article ID 3495432, 8 pages
https://doi.org/10.1155/2017/3495432

Research Article

Raman Spectroscopic Study of As-Deposited and Exfoliated Defected Graphene Grown on (001) Si Substrates by CVD

T. I. Milenov,[1] E. Valcheva,[2] and V. N. Popov[2]

[1]*"E. Djakov" Institute of Electronics, Bulgarian Academy of Sciences, 72 Tzarigradsko Chaussee Blvd., 1784 Sofia, Bulgaria*
[2]*Faculty of Physics, University of Sofia, 5 James Bourchier Blvd., 1164 Sofia, Bulgaria*

Correspondence should be addressed to T. I. Milenov; teddymilenov@abv.bg

Received 2 January 2017; Revised 15 March 2017; Accepted 10 April 2017; Published 27 June 2017

Academic Editor: Tino Hofmann

We present here results on a Raman spectroscopic study of the deposited defected graphene on Si substrates by chemical vapor deposition (thermal decomposition of acetone). The graphene films are not deposited on the (001) Si substrate directly but on two types of interlayers of mixed phases unintentionally deposited on the substrates: a diamond-like carbon (designated here as DLC) and amorphous carbon (designated here as αC) are dominated ones. The performed thorough Raman spectroscopic study of as-deposited as well as exfoliated specimens by two different techniques using different excitation wavelengths (488, 514, and 613 nm) as well as polarized Raman spectroscopy establishes that the composition of the designated DLC layers varies with depth: the initial layers on the Si substrate consist of DLC, nanodiamond species, and C_{70} fullerenes while the upper ones are dominated by DLC with an occasional presence of C_{70} fullerenes. The αC interlayer is dominated by turbostratic graphite and contains a larger quantity of C_{70} than the DLC-designated interlayers. The results of polarized and unpolarized Raman spectroscopic studies of as-grown and exfoliated graphene films tend to assume that single- to three-layered defected graphene is deposited on the interlayers. It can be concluded that the observed slight upshift of the 2D band as well as the broadening of 2D band should be related to the strain and doping.

1. Introduction

Graphene is a one-atom-thick layered material that consists of completely sp^2-bonded carbon atoms tightly packed into a honeycomb lattice. It has a lot of unique properties promising a huge number of possible applications (see, e.g., [1]). A lot of different ways of synthesizing graphene were experimentally tested during the last decade; however, only thermally and plasma-assisted chemical vapor deposition (CVD/PECVD) on metal substrates (copper, nickel, etc.) [2, 3] as well as epitaxial growth on SiC substrates and so on [4, 5] were developed for industrial application. The latter method is based on C (or Si) termination of the $(0001)_C$ (or $(0001)_{Si}$) SiC surface and requires high temperature and expensive SiC substrates. The CVD method is based on the plasma-enhanced thermal decomposition of a carbon-containing precursor on a catalytic metal surface. This method provides high reliability and relatively high quality of graphene films, and now, there are a lot of suppliers of reactors for PECVD of graphene. The most preferred precursor is methane (CH_4) as the chemical bond in CH_4 is relatively strong and prevents fast decomposition of the reagent at temperatures below 1000°C (see, e.g., [6]). However, production for microelectronic applications requires transfer of the graphene layers on an insulating surface and, consequently, a large number of additional defects affecting the properties of graphene can be introduced. Therefore, the problem with the deposition of graphene on silicon (or surfaces compatible with silicon technology such as SiO_2) still remains unsolved. We demonstrated the possible application of acetone as a precursor in a thermally assisted CVD and showed that few-layered defected graphene/folded graphene can be deposited on commercially available metal foils—Ni, ($Cu_{0.5}Ni_{0.5}$), μ-metal, and stainless steel SS 304 in a recently published work [7]. Further, we established (see [8]) by Raman spectroscopy, scanning electron microscopy (SEM), X-ray diffraction (XRD), and grazing incidence X-ray diffraction (GIXRD) as well as by X-ray photoelectron spectroscopy

(XPS) the presence of single- to few-layered defected graphene on two different types of interlayers deposited on (100) Si surface: (i) a diamond-like carbon (DLC) layer with some SiC contents (in the range below 5w%) and some residual quantities of SiO_2, and (ii) a complex amorphous carbon layer consisting of a mixture of sp^2- and sp^3-hybridized carbon as well as very small amount of fullerenes, SiO, and so on.

Here, we focus our experimental study on the Raman spectroscopic characterization of defected as-deposited graphene layers (including polarized spectroscopy) as well as graphene flakes exfoliated from similar specimens by two different ways using 488, 514, and 633 nm excitation laser wavelengths aiming at unambiguous confirmation of the graphene deposition of as well as the identification of the exact composition of the interlayers between the Si substrate and graphene layer/s.

2. Experimental

2.1. CVD Process. We use 2 inches in diameter (001) Si substrates and a horizontal tube quartz CVD reactor with an internal diameter of approximately 70 mm. The experimental setup also consists of a gas-supply system (inlet and outlet parts), a thermostat with acetone evaporation alert/indication system, a quartz substrate holder, and a resistive heating furnace. The CVD process is based on thermal decomposition of acetone in Ar main gas flow. The deposition temperature was in the range 1150–1160°C. The temperature of the thermostat was kept at 12°C. In order to prevent the supersaturation in the high-temperature zone of the reactor, we used a "pulsed" regime in experiments by alternating the flow of the gas mixture of Ar + C_3H_6O) for 3 min on top of the main flow of pure Ar of about 150–180 cm^3/min for 1.5 min for each pulse. The optimal results (predominantly single-layered graphene) were obtained after two deposition pulses.

2.2. Exfoliation. We exfoliated the carbon films deposited on (001) Si substrates by the following two different techniques:

(i) The Scotch tape method (see, e.g., [9]): we put tightly the adhesive Scotch tape on the multilayered graphene side of the specimens. After peeling the tape off the specimen, a single- to few-layered graphene remains on the tape's surface and the interlayer between the upper few layers of graphene and the substrate becomes accessible for spectroscopic examination. Then, we put tightly the Scotch tape with graphene flakes either on 320 nm SiO_2/Si or on glass substrate. About 30–50% of the graphene flakes remain adhered to the SiO_2 or glass substrate after removing the tape due to the Van der Waals force.

(ii) We also adhered the multilayered graphene side of the specimens to epoxy resin. After careful cleavage, the most part of the graphene layer/s remains on the surface of the resin. Then, the adhered to the resin graphene film becomes accessible for spectroscopic examination. The Raman spectrum of the epoxy resin does not contain strong peaks around the 2D band of graphene (the area around 2630–2670 cm^{-1}). We established that the 2D band of graphene is clearly distinguishable for graphene regions lying on gas bubbles close to the surface of the resin; otherwise, the 2D band of graphene is weak.

2.3. Characterization. The Raman measurements were carried out in backscattering geometry at a micro-Raman HORIBA Jobin Yvon Labram HR 800 visible spectrometer equipped with a Peltier-cooled CCD detector with a He-Ne (633 nm wavelength and 0.5 mW) laser excitation. The 514 nm (about 23 mW) as well as 488 nm (about 24 mW) lines of an external Ar laser were also used. The laser beam was focused on a spot of about 1 μm in diameter, the spectral resolution being 0.5, 0.7, and 1 cm^{-1}, respectively, or better.

The Raman spectrum of graphene is a clearly established fingerprint of this 2D material (see [10]). The main first-order features in the Raman spectra of graphene and defect-infested graphene excited at 633 nm wavelength are the following:

(i) G band (~1582 cm^{-1}) is the only band in graphene allowed by selection rules for first-order Raman effect; it is ascribed to optical (iTO and LO) doubly degenerate phonons of E_{2g} symmetry at the Γ point (initially described by Tuinstra and Koenig [11]).

(ii) D band (~1330 cm^{-1}) is due to breathing-like bands of C hexagonal rings (corresponding to transverse optical phonons near the K point) and requires a defect for its activation via an intervalley double-resonance Raman process (see [12]).

(iii) D' band (at about 1615 cm^{-1}; defect induced similarly to the D band) occurs via an intravalley double-resonance process (see, e.g., [13]).

(iv) D" band (at about 1145 cm^{-1}) is resulting from double-resonance intervalley scattering of LA phonons on defects (see [14]). The intensity of this band should be about 100 times lower than that of the D band.

Overtones and combination bands:

(i) 2D band (historically known from graphite and carbon nanotube-related literature as G'- peak) appears at about 2648–2665 cm^{-1}. It is clearly shown [15–20] that the shape and width of the 2D band can be used for the identification of the mono-, bi-, and three-layered graphene.

(ii) The overtone of the D'- peak (2D') and combination G^* (G^* = (iTA + LA) phonons), as well as (D+D') bands, occur around 3230, 2450, and 2930 cm^{-1}, respectively (see [21]).

3. Results and Discussion

Two areas with different surface morphologies are observed by optical microscopy (Figure 1(a)): a clear relief (ridge-like

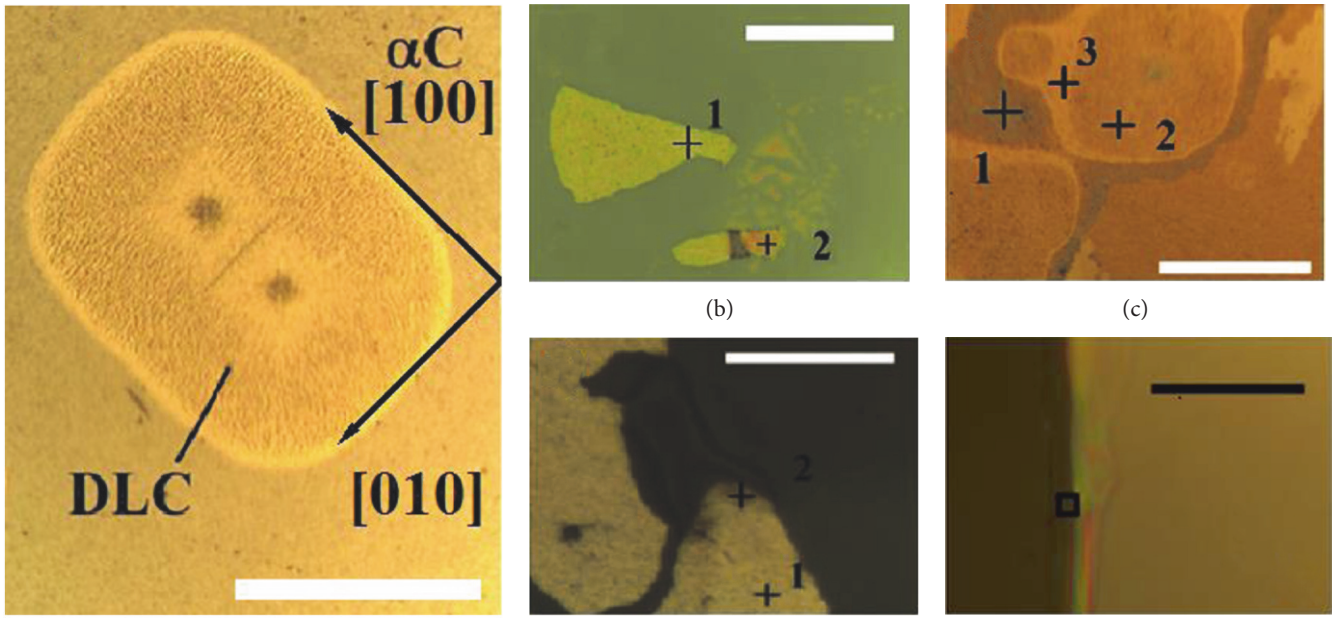

Figure 1: Optical microscopy image of the surface morphology of (a) as-deposited graphene and graphene-related phases on diamond-like carbon (DLC) and amorphous carbon (αC) interlayers. The arrows remarked [100] and [010] directions of the Si substrate. The marker represents 20 μm. (b) The exfoliated and transferred graphene flakes on 320 nm SiO_2. The Raman spectra are taken from "+"-marked positions. The marker represents 30 μm. (c) The layers remaining on the surface of the substrate after exfoliation by Scotch tape. The Raman spectra are taken from the "+"-marked positions near points 1, 2, and 3. The marker represents 30 μm. (d) The exfoliated and transferred graphene flakes on glass substrate. The Raman spectra are taken from the "+"-marked positions near points 1 and 2. The marker represents 20 μm. (e) A graphene flake on air bubble near the epoxy resin surface. The Raman spectra are taken from the square-marked position. The marker represents 20 μm.

formations) lying along <001> directions covers the first area denoted as DLC while the second area (denoted as αC) is covered by an inhomogeneous film with a constant depth. It should be also mentioned that optical inhomogeneities are observed on the DLC as well as αC-marked areas.

It should be recalled that the Raman spectrum (excited at 633 nm laser wavelength) taken from αC- and DLC-denoted areas (see [8]) contains all features typical for graphene: symmetric and clearly pronounced 2D band with full width at a half maximum (FWHM) of 40–56 cm^{-1}, I_{2D}/I_G ratio between 2 and 3.5, and I_{2D}/I_D ratio between 2 and 4. However, the 2D band appears at about 2660–2668 cm^{-1} (for single- and bilayered graphene, respectively), that is, it is blueshifted by about 20 cm^{-1} relative to the results presented in [15, 22, 23].

Due to the double-resonance origin of most of the monitored spectral features, we perform a Raman spectroscopy examination of as-deposited defected graphene at 488, 514, and 633 nm excitation wavelengths and the results are presented in Figure 2. The 2D bands are blueshifted by about 20 cm^{-1} and can be typically deconvoluted into (a) a single Lorentzian with FWHM of about 40-41 cm^{-1} (see Figure 3(a)); (b) four Lorentzians (FWHM of 22 (±1) cm^{-1}) for 2D band with total width of 45–56 cm^{-1} (see Figure 3(b)); and (c) six Lorentzians (Figure 3(c)) for 2D band with total width larger than 56 cm^{-1}. The results of the deconvolution indicate the presence of single-, bi-, and three-layered defected graphene, respectively (see [15–20]). We did not establish a clear difference between the

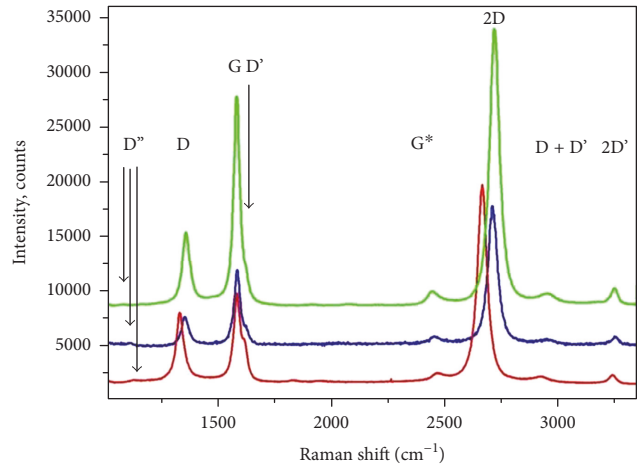

Figure 2: Raman spectra taken from as-grown films excited at 633 nm (red trace), 514 nm (blue trace), and 488 nm (green trace) laser wavelengths.

graphene layers deposited on αC and DLC interlayers; however, bi- and three-layered areas were more frequently observed on DLC interlayers. The results for predominantly single-layered (SL) and bilayered (BL) defected graphene (according to the deconvolution of 2D bands) are summarized in Table 1.

In order to access the interlayers as well as graphene flakes for Raman examination, the so-called Scotch tape

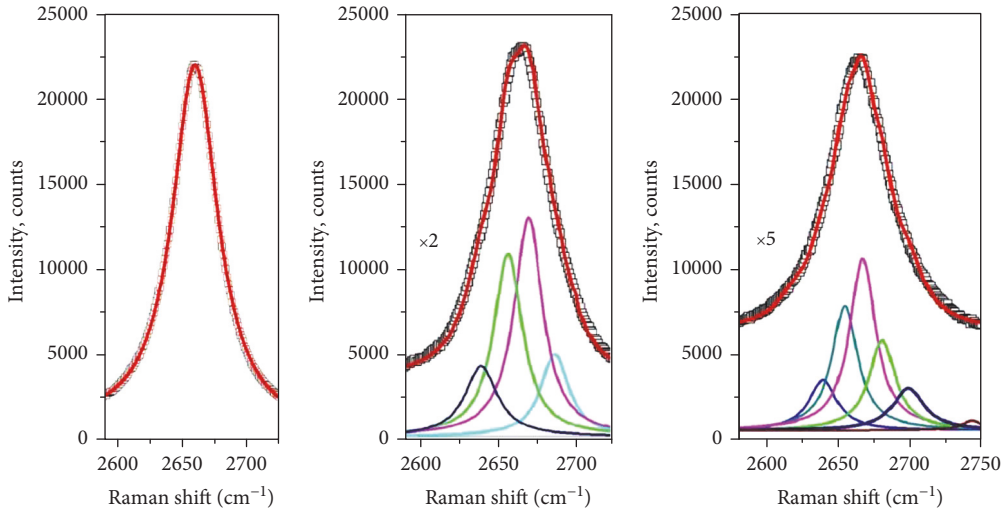

Figure 3: Deconvolution of 2D band identified as coming from single-layered (a), bilayered (b), and three-layered defected graphene deposited on αC. The spectrum is excited at 633 nm laser wavelength.

Table 1: Summarized results of Raman spectroscopy examination of as-deposited defected graphene films.

Excitation wavelengths	D band, cm^{-1}	G band, cm^{-1}	2D band, cm^{-1}	FWHM 2D Band, cm^{-1}; assignment
488 nm	1358	1581	2717	40–42; SL 48–54; BL
514 nm	1353	1582	2707	40–42; SL 48–54; BL
633 nm	1330	1581	2660	40–42; SL 48–54; BL

method was initially used for exfoliation. The Raman spectra of the graphene flakes exfoliated in this way with some occasional amorphous (αC) interlayers transferred to Si/SiO_2 (300 nm) or glass substrate are shown in Figures 4 and 5, respectively.

A lot of flakes (of the order of 10^2) were transferred on Si/SiO_2 and examined by Raman spectroscopy. The Raman spectra are enhanced due to interference effects caused by the SiO_2 300 nm layer over the Si substrate, and I_{2D}/I_G varies in the range 3.5-6.0. However, it was impossible to isolate single-layered graphene flake (or to obtain clear Raman response of single-layered graphene) in this way. The exfoliated flakes were never transparent (see point 1 in Figure 1(b)). The best spectra were recorded from the points in a darker contrast (point 2 in Figure 1(b)), but the FWHM of 2D Raman band remains >35 cm^{-1}. Moreover, the D" band slightly overlaps with the second order of Si substrate when the spectrum is excited at 514 as well as 488 nm laser wavelengths.

After peeling the tape off the specimen, the interlayer between the upper flake and the substrate is accessed. The remaining interlayers have different optical contrasts (see Figure 1(c)) and Raman spectra: the spectrum of typically

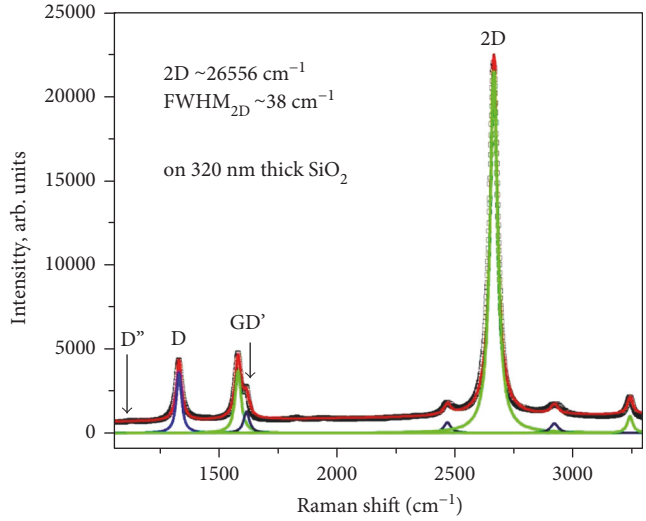

Figure 4: The Raman spectrum of defected 1-2-layered graphene transferred on 320 nm SiO_2. The 2D band is symmetric and appears at 2658-2659 cm^{-1} with FWHM of 38–40 cm^{-1} (measured in point 2) and 40–42 cm^{-1} (measured in point 1).

retained interlayer (point 1 in Figure 1(c)) in Figure 5 is very similar to that of turbostratic graphite (see [24]), but weak peaks of C_{70} fullerenes (the features observed at about 1450 and 1530 cm^{-1} (see [25, 26])) are also clearly distinguished (Figure 5). The strong modes of fullerenes C_{70} at about 1180 and 1568 cm^{-1} are merged with D" and G bands.

The Raman spectra (Figure 6) taken from points 2 and 3 (Figure 1(c)) are similar as they contain the most prominent modes of C_{70} peaks at 1160, 1220, 1454, 1526, and 1565 cm^{-1} [25, 26], nanodiamond (Nd) peaks at 1330 and 1620 cm^{-1} (see [27]), and turbostratic graphite. The D, G, and D' bands are found at 1335, 1590, and 1612 cm^{-1}, respectively, but in a different proportion: the spectrum from point 3 is dominated

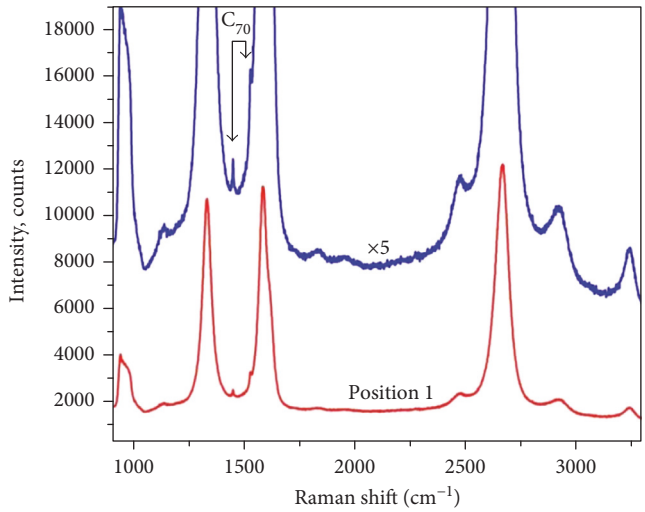

Figure 5: The Raman spectrum of the interlayer (point 1, Figure 1(c)) of αC after exfoliation by Scotch tape. The features observed at about 1450 and 1530 cm^{-1} are typical for C_{70} fullerenes.

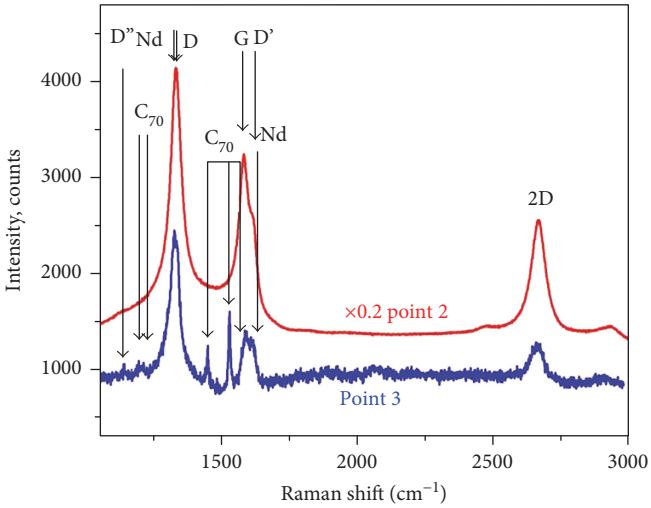

Figure 6: Raman spectra of the interlayer that remains on the substrate after exfoliation by the Scotch tape method taken from points 2 and 3 (Figure 1(c)).

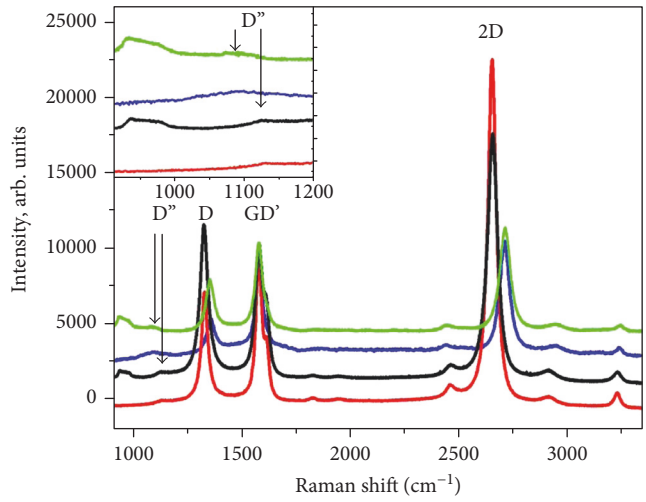

Figure 7: The Raman spectra of as-grown graphene on αC excited at 488 nm (green trace) and 633 nm (black trace) wavelengths. The similar spectra of exfoliated graphene transferred on a glass substrate excited at 488 nm (blue trace) and 633 nm (red trace). The inset: magnified part of the region 900–1200 cm^{-1}.

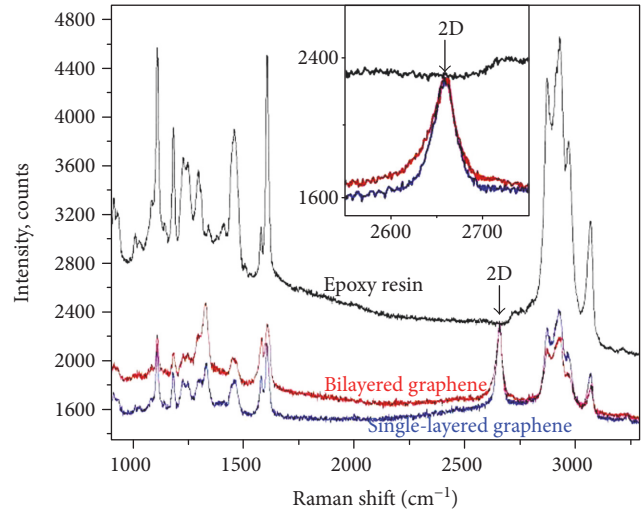

Figure 8: Raman spectra of graphene films situated on air bubbles/cavities. The 2D band is situated at 2655 cm^{-1} and has FWHM ~28 cm^{-1} (i.e., it corresponds to single-layered graphene—blue trace).

by the peaks of C_{70} and Nd while the spectrum from point 2 is dominated by turbostratic graphite (see Figure 6). It should be also remarked that features of C_{60} fullerenes (see, e.g., [25, 26]) were not observed.

As it was mentioned above, the D" band overlaps with the second-order band of Si substrate especially when the spectrum is excited at 488 and 514 nm laser wavelengths. In order to distinguish the dispersion of the D" band of several Scotch tape methods, exfoliated flakes were transferred on glass substrates. The flakes have very similar surface morphology to those transferred on SiO_2/Si substrates (Figure 1(d)). The Raman spectrum of such flakes is not significantly different from that of the as-deposited layers (Figure 7); however, the D" band appears at 1096 (for 488 nm excitation) and at 1135 cm^{-1} (for 633 nm excitation), respectively, that is, they coincide with the data of Herziger et al. [14].

According to the above results, we conclude that the exfoliation by the Scotch tape method does not enable splitting up between the defected graphene and the interlayers (especially the αC-designated one). Another way for exfoliation was probed (by exfoliation on epoxy resin), and the optical micrograph image of the area of the edge of a resin bubble and the Raman spectrum taken from this area (excited at 633 nm) are shown in Figures 1(e) and 8, respectively. The Raman spectrum of epoxy resin does not contain any features in the 2D region of graphene (upper

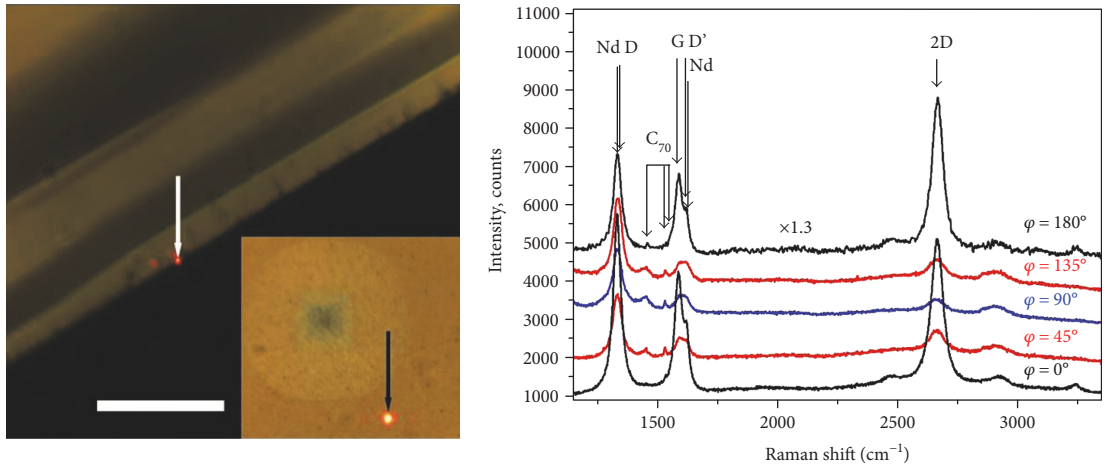

(a) (b)

FIGURE 9: (a) Optical photography of the specimen in $X(YY)X$ geometry (in Porto notations). The inset: optical photography of the specimen in $Z(YY)Z$ geometry (in Porto notations). The arrow-remarked laser spots are eye guide showing the real area of the laser spot during measurements. The marker represents 10 μm. (b) Spatially resolved Raman spectra of as-deposited defected graphene at 633 nm excitation.

trace in Figure 8); hence, 2D bands of a single- and bilayered graphene were identified at the edge of a lot of bubbles on the surface of the resin (Figure 1(e)). It should be clearly remarked that the measured FWHM of the 2D band of such single-layered graphene is about 27–29 cm^{-1}, but it is situated at 2654–2656 cm^{-1}, that is, it remains upshifted with about 10–15 cm^{-1}.

Recently, Li et al. [28] established that the intensity of 2D band varies as a cosine to the fourth power when the laser propagation direction is parallel to the graphene layer and the polarization is rotated around it. They also derived the orientation distribution function of monolayered graphene as well as that of graphene paper and highly oriented pyrolytic graphite. We perform similar measurements in $X(Y_\varphi Y_\varphi)X$ geometry, φ being the angle between the incident laser beam polarization and the graphene layer plane; Z is the axis perpendicular to the graphene plane, and the laser beam propagates transversely to the graphene layer along the X direction (see Figure 9(a)). The excitation laser beam was focused in a manner to comprise no more than 30% of the edge of the Si substrate and graphene film (Figure 9(a)). The parallel scattering geometry was used. The measurements were performed starting from $\varphi = 0^\circ$ (corresponding to $X(YY)X$ in Porto notations) and finished at $\varphi = 180^\circ$. The preliminary results of these rotational angle-dependent Raman measurements of as-deposited specimen are presented in Figure 9. The signal significantly drops upon changing the angle from 0° to 90° and increases again in the interval between 90 and 180° which resembles indeed the $\cos^4$ law. At 90° (corresponding to $X(ZZ)X$ in Porto notations), the Raman signal is very weak but still observable (Figure 9), and the rotational angle-independent features of C_{70} fullerenes and nanodiamond (Nd) dominate the spectrum. The residual features in the Raman spectra taken at $\varphi = 90^\circ$ point out that the measured polarized Raman spectra are taken from graphene deposited on DLC interlayer. The measurements in this scattering geometry ($X(YY)X$ in Porto notations) access measurements of the interlayer/s without exfoliation. On the other hand, the polarized Raman study confirms the deposition of graphene because the intensities of the most prominent Raman features of graphite (D, G, and 2D bands) show similar behavior in similar conditions as those of graphene. However, the intensity of the Raman features of graphene decreases significantly slower than those of graphene as it is shown in [28].

It is worth noting that the 2D band from the single-layered graphene regions is symmetric and strong, but it is somewhat broadened with FWHM of about 40–42 cm^{-1} and is blueshifted by 15–20 cm^{-1} in as-grown specimens. It is well known that such behavior is usually related to strain (see [29–32]) and doping [33]. Moreover, Lee et al. [34] and Bouhafs et al. [35] experimentally studied the influence of these parameters on the position and FWHM of G and 2D bands in single- and bi-/multilayered graphene, respectively. The deduced simple plot of the 2D versus G band positions enables distinguishing the influence of doping and strain on the positions of G and 2D bands. In our single-layered specimens, the G band is slightly uphifted by 1-2 cm^{-1} while the 2D band is more significantly blueshifted and broadened by 10–20 cm^{-1}. Therefore it can be assumed that the 2D band blueshift and broadening are due to the lattice strain predominantly as well as to the doping. It can be suggested that the lattice strain is due to the bonding between graphene and the interlayers while the doping should be related to charge transfer from the interlayers/interfaces to graphene as well as to different intrinsic (grain boundaries, etc.) and extrinsic (trapped nitrogen, oxygen, and impurities during the deposition) defects, that is, it can be related to the influence of the interlayers/substrates as well as of the deposition process.

4. Conclusions

We extended the analysis of defected graphene deposited by CVD as well as the two types of interlayers between the defected graphene layer/s and Si substrates by both

unpolarized and polarized Raman spectroscopy. The performed Raman spectroscopy examination of as-deposited defected graphene at 488, 514, and 633 nm excitation wavelengths enables the most of the monitored spectral features of double-resonance origin (D, D", and 2D bands). The Raman studies of exfoliation by the so-called Scotch tape method revealed that (a) the composition of the designated DLC interlayers varies with depth: the initial layers on the Si substrate consist of a mixed phase of turbostratic graphite, nanodiamond/diamond-like carbon, and C_{70} fullerenes while the upper ones are dominated by diamond-like carbon and some C_{70} fullerenes and (b) the amorphous carbon interlayer is dominated by turbostratic graphite and contains a larger quantity of C_{70} than the DLC-designated interlayers. Single- and bilayered defected graphene flakes were exfoliated on epoxy resin. The preliminary results of polarized Raman experiments show that the intensity of the 2D band varies as a cosine to the fourth power when the laser propagation direction is parallel to the graphene layer and the polarization is rotated around it which is an additional indication of the deposition of single-layered graphene. The results of Raman spectroscopic studies of as-grown and exfoliated graphene films tend to assume that the observed slight upshift of the 2D band as well as the broadening of 2D band is due to the strain and can be related to the bonding between the graphene and the interlayers, that is, it could be regarded as an influence of the interlayers between the defected graphene and the Si substrates.

Conflicts of Interest

The authors declare that there is no conflict of interest regarding the publication of this paper.

References

[1] A. Ferrari, F. Bonaccorso, V. Fal'ko et al., "Science and technology roadmap for graphene, related two-dimensional crystals, and hybrid systems," *Nanoscale*, vol. 7, pp. 4598–4810, 2015.

[2] K. S. Kim, Y. Zhao, H. Jang et al., "Large-scale pattern growth of graphene films for stretchable transparent electrodes," *Nature*, vol. 457, pp. 706–710, 2009.

[3] A. Reina, X. Jia, J. Ho et al., "Large area, few-layer graphene films on arbitrary substrates by chemical vapor deposition," *Nano Letters*, vol. 9, pp. 30–35, 2009.

[4] C. Berger, Z. Song, T. Li et al., "Ultrathin epitaxial graphite: 2D electron gas properties and a route toward graphene-based nanoelectronics," *The Journal of Physical Chemistry*, vol. 108, pp. 19912–19916, 2004.

[5] C. Berger, Z. Song, T. Li et al., "Electronic confinement and coherence in patterned epitaxial graphene," *Science*, vol. 312, pp. 1191–1196, 2006.

[6] R. Muñoz and C. Gómez-Aleixandre, "Review of CVD synthesis of graphene," *Chemical Vapor Deposition*, vol. 19, pp. 297–322, 2013.

[7] T. I. Milenov, I. Avramova, E. Valcheva, and S. S. Tinchev, "Deposition of graphene/graphene-related phases on different substrates by thermal decomposition of acetone," *Optical & Quantum Electronics*, vol. 48, p. 135-1-12, 2016.

[8] T. I. Milenov, I. Avramova, E. Valcheva et al., "Deposition of defected graphene on (001) Si substrates by thermal decomposition of acetone," *Superlattices and Microstructures*, In press.

[9] K. S. Novoselov, D. Jiang, F. Schedin et al., "Two-dimensional atomic crystals," *PNAS*, vol. 102, pp. 10451–10453, 2005.

[10] A. C. Ferrari and D. M. Basko, "Raman spectroscopy as a versatile tool for studying the properties of graphene," *Nature Nanotechnology*, vol. 8, pp. 235–246, 2013.

[11] F. Tuinstra and J. L. Koenig, "Raman spectrum of graphite," *The Journal of Chemical Physics*, vol. 53, pp. 1126–1130, 1970.

[12] C. Thomsen and S. Reich, "Double resonant Raman scattering in graphite," *Physical Review Letters*, vol. 85, pp. 5214–5217, 2000.

[13] A. C. Ferrari, "Raman spectroscopy of graphene and graphite: disorder, electron–phonon coupling, doping and nonadiabatic effects," *Solid State Communications*, vol. 143, pp. 47–57, 2007.

[14] F. Herziger, C. Tyborski, O. Ochedowski, M. Schleberger, and J. Maultzsch, "Double-resonant LA phonon scattering in defective graphene and carbon nanotubes," *Physical Review B*, vol. 90, p. 245431-1-6, 2014.

[15] A. C. Ferrari, J. C. Meyer, V. Scardaci et al., "Raman spectrum of graphene and graphene layers," *Physical Review Letters*, vol. 97, pp. 187401–187404, 2007.

[16] L. M. Malard, M. A. Pimenta, G. F. Dresselhaus, and M. S. Dresselhaus, "Raman spectroscopy in graphene," *Physics Reports*, vol. 473, pp. 51–87, 2009.

[17] A. K. Gupta, T. J. Russin, H. R. Gutiérrez, and P. C. Eklund, "Probing graphene edges via Raman scattering," *ACS Nano*, vol. 3, pp. 45–52, 2009.

[18] Y. Hao, Y. Wang, L. Wang et al., "Probing layer number and stacking order of few-layer graphene by Raman spectroscopy," *Small*, vol. 6, pp. 195–200, 2010.

[19] S. Chen, W. Cai, R. D. Piner et al., "Synthesis and characterization of large-area graphene and graphite films on commercial Cu–Ni alloy foils," *Nano Letters*, vol. 11, pp. 3519–3525, 2011.

[20] J. U. Lee, N. M. Seck, D. Yoon, S. M. Choi, Y. W. Son, and H. Cheong, "Polarization dependence of double resonant Raman scattering band in bilayer graphene," *Carbon*, vol. 72, pp. 257–263, 2014.

[21] V. N. Popov and P. Lambin, "Theoretical polarization dependence of the two-phonon double-resonant Raman spectra of graphene," *European Physical Journal B*, vol. 85, p. 418, 2012.

[22] P. Klar, E. Lidorikis, A. Eckmann, I. A. Verzhbitskiy, A. C. Ferrari, and C. Casiraghi, "Raman scattering efficiency of graphene," *Physical Review B*, vol. 87, p. 205435-1-12, 2013.

[23] P. Poncharal, A. Ayari, T. Michel, and J.-L. Sauvajol, "Raman spectra of misoriented bilayer graphene," *Physical Review B*, vol. 78, p. 113407-1-4, 2008.

[24] P. H. Tan, C. Y. Hu, J. Dong, W. C. Shen, and B. F. Zhang, "Polarization properties, high-order Raman spectra, and frequency asymmetry between Stokes and anti-Stokes scattering of Raman modes in a graphite whisker," *Physical Review B*, vol. 64, p. 214301-1-12, 2001.

[25] K. A. Wang, P. Zhou, A. M. Rao, P. C. Eklund, R. A. Jishi, and M. S. Dresselhaus, "Intramolecular-vibrational-mode softening in alkali-metal-saturated C70 films," *Physical Review B: Condensed Matter*, vol. 48, pp. 3501–3506, 1993.

[26] P. M. Rafailov, V. G. Hadjiev, H. Jantoljak, and C. Thomsen, "Raman depolarization ratio of vibrational modes in solid C 60," *Solid State Communications*, vol. 112, pp. 517–520, 1999.

[27] S. Prawer, K. W. Nugent, D. N. Jamieson, J. O. Orwa, L. A. Bursill, and J. L. Peng, "The Raman spectrum of nanocrystalline diamond," *Chemical Physics Letters*, vol. 332, pp. 93–97, 2000.

[28] Z. Li, R. J. Young, I. A. Kinloch et al., "Quantitative determination of the spatial orientation of graphene by polarized Raman spectroscopy," *Carbon*, vol. 88, pp. 215–224, 2015.

[29] M. Mohr, J. Maultzsch, and C. Thomsen, "Splitting of the Raman 2 D band of graphene subjected to strain," *Physical Review B*, vol. 82, p. 201409-1-4 R, 2010.

[30] O. Frank, M. Mohr, J. Maultzsch et al., "Raman 2D-band splitting in graphene: theory and experiment," *ACS Nano*, vol. 5, pp. 2231–2239, 2011.

[31] V. N. Popov and P. Lambin, "Theoretical 2 D Raman band of strained graphene," *Physical Review B*, vol. 87, p. 155425-1-7, 2013.

[32] V. N. Popov and P. Lambin, "Theoretical Raman intensity of the G and 2D bands of strained graphene," *Carbon*, vol. 54, pp. 86–93, 2013.

[33] A. Das, S. Pisana, B. Chakraborty et al., "Monitoring dopants by Raman scattering in an electrochemically top-gated graphene transistor," *Nature Nanotechnology*, vol. 3, pp. 210–215, 2008.

[34] J. E. Lee, G. Ahn, J. Shim, Y. S. Lee, and S. Ryu, "Optical separation of mechanical strain from charge doping in graphene," *Nature Communications*, vol. 3, p. 1024-1-8, 2012.

[35] C. Bouhafs, A. A. Zakharov, I. G. Ivanov et al., "Multi-scale investigation of interface properties, stacking order and decoupling of few layer graphene on C-face 4H-SiC," *Carbon*, vol. 116, pp. 722–732, 2017.